A simple surface water biogeochemical model
1. Description, sensitivity analyses, and idealized simulations

Paul W. Jewell

Department of Geology and Geophysics, University of Utah, Salt Lake City

Abstract. Accurate simulation of surface productivity, dissolved nutrient and oxygen concentrations, and particulate carbon flux are critical components of any viable surface water quality model. A linear, three-component model consisting of a dissolved limiting nutrient, phytoplankton, and zooplankton coupled to a one-dimensional turbulence closure fluid flow model has been constructed and applied to a generalized surface water setting. The model transfers nutrients from the euphotic zone to the subeuphotic zone using empirical biogenic flux-depth relationships. The model does not require specification of biogenic particle settling velocity which is known to vary by at least 2 orders of magnitude in natural surface waters and thus constitutes a major source of uncertainty in many biogeochemical models. Using an empirical biogenic flux-depth function to transfer nutrients through the water column introduces spatial errors which are most extreme in deep water. The model is thus most appropriate for lakes, estuaries, and shallow (<1000 m deep) marine settings. Restricting the model to three components with seven empirical constants permits a high degree of computational efficiency. Sensitivity analyses of the empirical constants show that integrated surface productivity is responsive to the three constants related to light (initial slope of the light-productivity curve, light attenuation coefficient of the water, and photosynthetically available radiation) while being relatively insensitive to constants which are strictly related to biogeochemical transformations (remineralization rate, nutrient half-saturation constant, maximum zooplankton growth rate, and Ivlev constant for zooplankton growth). Model simulations using idealized surface temperature boundary conditions produce thermal and biogeochemical characteristics of a typical temperate-latitude lake. The simulations also suggest that vertical mixing plays an important role in producing the late seasonal, deep chlorophyll maximum commonly observed in many surface water settings.

Introduction

The biogeochemical cycles of surface water are a key component to understanding many important processes in Earth science and environmental engineering. Nutrients are consumed in the euphotic zone by phytoplankton which are then cycled through a food chain. Organic detritus and fecal material from the food chain settles through the water column where it is remineralized into dissolved organic and inorganic constituents. Oxygen is consumed during the course of this subeuphotic zone remineralization. A small fraction of the particulate organic carbon flux becomes permanently sequestered in bottom sediments. These processes have been studied in the field, in the laboratory, and with numerical models over the past few decades. An overview of previous numerical models is provided here as a prelude to the model described in this paper.

Aquatic biogeochemical models which simulate photosynthesis-respiration processes vary enormously. The most simple and direct are box models in which various spatial compartments are linked by a physical mixing mechanism. Box models of oxygen and nutrients have been effectively applied to the

world ocean [*Broecker*, 1974; *Sarmiento et al.*, 1988a; *Shaffer*, 1989], borderland marine basins [*Sarmiento et al.*, 1988b], coastal upwelling [*Jewell*, 1994a, b], and lakes [*Imboden*, 1974]. Time-dependent modeling of various components adds additional sophistication to standard box models [e.g., *Snodgrass and O'Melia*, 1975; *Higgens and Kim*, 1982; *Gachter and Imboden*, 1985].

Multicomponent ecosystem models allow a measure of sophistication not possible with simple box models by considering the time-dependent interaction between specific biological components (e.g., phytoplankton, zooplankton, bacteria, organic detritus, nutrients). The various biogeochemical components are linked by a variety of rate constants [e.g., *Harleman*, 1977; *Jamart et al.*, 1977; *Kremer and Nixon*, 1978; *Fasham et al.*, 1990]. The coupled, nonlinear nature of these models necessitates the use of a numerical algorithm such as Runge-Kutta for solving the simultaneous differential equations [e.g., *Fasham et al.*, 1990].

Fluid physics is one of the primary controls of aquatic biogeochemical processes and must therefore be incorporated into any realistic ecosystem model. Empirical models have related the stability of the water column to biogeochemical processes [*Pingree et al.*, 1978; *Platt*, 1972; *Falkowski and Wirick*, 1981]. Fluid flow numerical models of one or more spatial dimensions are often coupled to ecosystem models to accurately simulate dissolved and particulate biogeochemical con-
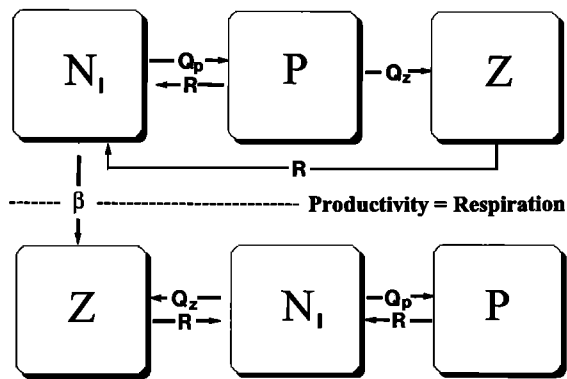
Figure 1. Diagrammatic representation of the three-component biogeochemical model. Letters refer to symbols in (1)–(3).

centrations. Finite difference, fluid flow models of simplified nutrient cycles have been used to study vertical profiles of nutrients and oxygen in the open ocean and lakes. The simplest of these models considers only a particulate form of carbon [*Peterson and Festa*, 1984]. Additional sophistication is obtained by adding a dissolved form of the limiting nutrient and dissolved oxygen [*Southam et al.*, 1982; *Jewell*, 1992]. The water quality analysis simulation program (WASP) developed by the U.S. Environmental Protection Agency solves a one-dimensional (horizontal) formulation of the shallow water equations in conjunction with a multicomponent biogeochemical model [*Ambrose et al.*, 1993]. The WASP program is designed for application to rivers and well-mixed estuaries.

Much recent research has been directed toward coupling primitive equation, three-dimensional general circulation models to various types of biogeochemical models [*Maier-Reimer and Hasselman*, 1987; *Wroblewski et al.*, 1988; *Bacastow and Maier-Reimer*, 1990, 1991; *Najjar et al.*, 1992]. The most sophisticated of these models have used complete ecosystem formulations to study entire ocean basins [*Fasham et al.*, 1993; *Sarmiento et al.*, 1993] or specific mesoscale domains [*Walsh*, 1975; *Wroblewski*, 1977; *Walsh et al.*, 1988; *Hofmann*, 1988]. While the sophistication inherent in these models is often necessary to provide complete spatial coverage of phytoplankton, zooplankton, bacteria, and other biogeochemical components, they are computationally intensive and can often only be run on state-of-the-art, array-processing computers by a small number of research organizations.

There are a variety of applications for which complete, three-dimensional coverage of the aquatic regime is necessary, yet a complete aquatic ecosystems model is not required. Examples include the spatial distribution of carbon flux to the sediments in marine and terrestrial environments, the controls of bottom water eutrophication by various physical forcings (e.g., wind, river water inflow), and the response of surface productivity to point source and nonpoint source nutrient loading. In these situations, simulations of specific sizes and forms of phytoplankton, zooplankton, and bacteria may be unnecessary. A simplified biogeochemical model based on sound assumptions represents a cost-effective alternative to complete, but computationally intensive, ecosystem models. Not only must fewer conservation equations be solved, but the biogeochemical model does not require nonlinear equation solvers (e.g., Runge-Kutta) which are often employed in other biogeochemical models.

The biogeochemical model described here is meant to evaluate the feasibility of using a simple, three-component biogeochemical model to simulate nutrients and surface productivity in conjunction with an empirical function for transferring nutrients between the euphotic and subeuphotic portions of the water column. *Wroblewski et al.* [1988] describe a similar three-component model coupled to an oceanic general circulation model, although their model does not specifically transfer nutrients through the water column and is meant to model the surface layer of entire ocean basins.

Initial simulations involve coupling the three-component biogeochemical model to a one-dimensional, turbulence closure fluid dynamic model. In this paper the model is described, sensitivity analyses are performed, an idealized simulation is presented, and specific relationships between water column physics and biogeochemistry are discussed. In the second paper of this study [*Jewell*, this issue], the one-dimensional model is applied to four well-studied yet diverse marine and lacustrine settings. The three-component, one-dimensional model has been developed as a prelude to more ambitious, computationally intensive, three-dimensional simulations of nutrient loading in lakes, the response of productivity and carbon flux to physical forcings in coastal upwelling zones, and a variety of other research topics.

Model Description

The biogeochemical model presented here rests on the premise that the water column can be separated into two parts: the euphotic zone where dissolved nutrients are transformed into particulate organic matter and cycled through a surface ecosystem and the subeuphotic zone where remineralization of the particulate matter dominates (Figure 1). The boundary between the two domains is known as the "compensation depth" and is defined as the point at which photosynthesis equals respiration [*Parsons et al.*, 1984]. This model differs from most previous ecosystem models in that the transfer of nutrients from the euphotic to the subeuphotic zone is accomplished by empirical biogenic flux-depth relationships [*Suess*, 1980; *Martin et al.*, 1987; *Berger et al.*, 1989, *Bishop*, 1989] rather than specification of a vertical settling velocity for biologically produced particles. Particle settling velocity is a feature of most previous ecosystem models, yet this parameter is known to range between 0 and 1000 m/d [*Smayda*, 1970]. Although data used to construct empirical biogenic flux-depth relationships show considerable scatter [e.g., *Bishop*, 1989], their use in this model is believed to represent a considerable improvement on the single settling velocity models. Although the biogenic flux-depth relationships have been exclusively derived from marine settings, there is no reason to believe they are not generally applicable to lakes. The exact form and application of these relationships are discussed in detail below.

Biogeochemical Equations

The three-component biogeochemical model consists of a dissolved, limiting nutrient, N_l; phytoplankton, P; and zooplankton, Z. The three components are coupled in linear fashion in both the euphotic and the subeuphotic zones (Figure 1). Conservation of the three biogeochemical components is described as a series of source and sink terms:

$$\frac{\partial N_l}{\partial t} = (-Q_p + R)P + RZ - \beta_e \quad 0 \le z < z_e \quad (1a)$$

$$\frac{\partial N_I}{\partial t} = (-Q_p + R)P + RZ \qquad z_e \le z < H \quad (1b)$$

$$\frac{\partial P}{\partial t} = (Q_p - R)P - Q_z Z \qquad 0 \le z < H \quad (2)$$

$$\frac{\partial Z}{\partial t} = (Q_z - R)Z \qquad 0 \le z < z_e \quad (3a)$$

$$\frac{\partial Z}{\partial t} = (Q_z - R)Z + \beta_s \qquad z_e \le z < H \quad (3b)$$

Q_p is phytoplankton growth rate; Q_z is zooplankton growth rate; and R is the remineralization rate. Here β_e and β_s are expressions for redistribution of nutrients in the euphotic and subeuphotic zones, respectively and are described in detail below; z_e is the compensation depth (i.e., the point at which $Q_p = R$); and H is total water depth. The chemical species and units for the biogeochemical components (N_I, P, and Z) are arbitrary but, of course, must be the same.

The amount of the Z component below the euphotic zone is being continually increased by the transfer function, β. In this sense the Z component assumes the role of both zooplankton and detritus found in more complicated ecosystem models [e.g., Harleman, 1977; Hofmann and Ambler, 1988; Fasham et al., 1990]. In nature, phytoplankton concentrations are generally orders of magnitude higher in the euphotic zone than in deeper water. As a result, Q_z in the subeuphotic zone is very small, and (3b) is essentially an expression for particulate organic detritus rather than zooplankton.

Although dissolved oxygen is not modeled in this study, it would be relatively simple to model oxygen as a component which is produced by photosynthesis, consumed by respiration, and coupled to dissolved nutrient concentrations by simple Redfield-type stoichiometry [e.g., Southam et al., 1982; Jewell, 1992]. Oxygen is not modeled in this study because much of the oxygen consumption in the lower portions of shallow lacustrine and marine settings is the result of flux into the sediments. Previous studies of dissolved oxygen with the one-dimensional turbulence closure model described below suggest that the calculated vertical mixing rates produced by the model in the lower portion of the water column are too small [Jewell, 1992]. Since the focus of this study is biogeochemical processes in surface waters where oxygen is often close to saturation, dissolved oxygen simulations were not undertaken.

Photosynthesis, respiration, and grazing. The expressions for the source and sink terms in (1)–(3) have been derived from a variety of previous aquatic ecosystem models. Phytoplankton growth rate, Q_p, is expressed as a function of light and nutrient limitation:

$$Q_p = Q_{max} \frac{\alpha I}{(Q_{max}^2 + \alpha^2 I^2)^{1/2}} \left(\frac{N_I}{K_p + N_I} \right) \quad (4)$$

Q_{max} is the maximum phytoplankton growth rate; I is light intensity; α is initial slope of growth rate versus light intensity; and K_p is the half-saturation constant for phytoplankton growth. The first factor in (4) represents the dependence of phytoplankton growth on light [Smith, 1936; Parsons et al., 1984]. The second factor represents Michaelis-Menten nutrient limitation kinetics [Michaelis and Menten, 1913; Monod, 1942; Parsons et al., 1984] and is a standard feature of most aquatic ecosystem models.

Maximum phytoplankton growth rate is expressed as a func-

tion of temperature according to the expression proposed by Epply [1972] on the basis of empirical data:

$$Q_{max} = 0.59 \exp{(0.0633T)} \quad (5)$$

T is temperature in degrees Celsius. Ecosystem model studies employing (5) include Kremer and Nixon [1978] and Fasham et al. [1990].

Light which penetrates the water column is attenuated as a function of depth according to the relationship

$$I(z) = (\text{PAR})I_0 \exp{\left(-k_w z - \int_z^0 k_c \, dz \right)} \quad (6)$$

$I(z)$ is depth-dependent light (units of watts per square meter). PAR is "photosynthetically available radiation," i.e., the amount of light actually used in photosynthesis [Parsons et al., 1984]. I_0 is surface light intensity (watts per square meter); k_w is the attenuation coefficient for pure water (units of m^{-1}); and k_c is the attenuation coefficient for organic matter [Parsons et al., 1984; Fasham et al., 1990]. Here k_c is modeled according to the relationship of Riley [1956].

$$k_c = 0.054 \text{ Chl-}a^{2/3} + 0.0088 \text{ Chl-}a \quad (7)$$

Chl-a is chlorophyll in units of milligrams per cubic meter. A commonly reported value for k_w in clear water is 0.04 [Jerlov, 1976; Parsons et al., 1984]. Lakes or coastal marine settings containing abundant organic or inorganic sediment have considerably greater values of k_w; application of this model to these types of settings is discussed in greater detail by Jewell [this issue].

Surface light is modeled according to an expression for incoming shortwave radiation [Parkinson and Washington, 1979]:

$$I_0 = \frac{S_c \cos^2 \theta (1.0 - 0.6C_l^3)}{10^{-5}(\cos \theta + 2.7)e_a + 1.085 \cos \theta + 0.10} \quad (8)$$

S_c is the solar constant (1353 W/m^2); $\cos \theta$ is the solar zenith angle; C_l is the fraction of cloud cover; and e_a is the atmospheric vapor pressure. The last variable is considered to be a constant (10^4 Pa) in this study, since its value does not change the computation of I_0 appreciably. The solar zenith angle is computed from standard astronomical formulations.

$$\cos \theta = \sin \phi \sin \delta + \cos \phi \cos \delta \cos \psi \quad (9)$$

Here ϕ is latitude; δ is the solar inclination angle; and ψ is the hour angle of the day. When θ is less than zero, I_0 is set to zero.

Although zooplankton growth rate can determined with an expression similar to the Michaelis-Menten expression for phytoplankton growth rate [e.g., Fasham et al., 1990], it is more typically determined with the Ivlev exponential relationship [Ivlev, 1945; Jamart et al., 1977; Kremer and Nixon, 1978; Hofmann and Ambler, 1988; Wroblewski et al., 1988].

$$Q_z = G_{max}[1.0 - \exp{(-K_I P)}] \quad (10)$$

G_{max} is the maximum zooplankton growth rate; K_I is the Ivlev constant; and P is phytoplankton concentration.

Productivity-depth relationships. Transfer of nutrients from the euphotic zone to the subeuphotic zone is accomplished with empirical biogenic flux-depth relationships established from observations in the ocean [Martin et al., 1987; Berger et al., 1989; Bishop, 1989]. These relationships have been developed from sediment trap data collected at more than 200

Table 1. Summary of Parameters Used in the Standard Biogeochemical Model

Parameter	Symbol	Value
Remineralization rate, d^{-1}	R	0.10
Nutrient half-saturation constant, $mmol\ N/m^3$	K_p	0.2 + 0.16N; 1.0 for N > 5[a,b]
Maximum growth rate for zooplankton, d^{-1}	G_{max}	0.20[b]
Ivlev constant, $m^3/mmol\ N$	K_I	1.5[a,c]
Initial slope of light-productivity curve, $d^{-1}/W\ m^{-2}$	α	0.025[d]
Photosynthetically active radiation, dimensionless	PAR	0.5[d]
Light attenuation, m^{-1}	k_w	0.04[e]

[a]*Jamart et al.* [1977].
[b]*Walsh* [1988].
[c]*Hoffman and Ambler* [1988].
[d]*Fasham et al.* [1993].
[e]*Jerlov* [1976].

sampling points, mostly from the upper 2000 m of the water column [*Bishop*, 1989]. Several relationships have been proposed (see summary in the work by *Bishop* [1989]). The best fit of observations for depths of <1000 m has been chosen for this study since this is the depth range over which the proposed model will be most applicable [*Berger et al.*, 1987]:

$$J(z) = 6.3PP/z^{0.8} \qquad (11)$$

J is organic carbon flux (g C m^{-2} yr^{-1}); PP is primary productivity (also g C m^{-2} yr^{-1}); and z is depth.

In this model, vertically integrated primary productivity, PP, is defined as

$$PP = \int_{z_e}^{0} Q_p rP\ dz \qquad (12)$$

where r is the stoichiometric ratio necessary to convert units for phytoplankton, P, to grams of C per cubic meter.

The total amount of nutrients added to the subeuphotic zone (equation (3b)) is calculated from the flux relationships of (11):

$$\beta_s = \sum_{k=k_e}^{k_H} (J_k - J_{k-1})/\Delta z_k \qquad (13)$$

Here k_e refers to the model grid point immediately below the compensation depth; k_H is the bottommost model grid point; and Δz_k is the vertical distance between the k and $k - 1$ grid point. If the compensation depth is greater than the water depth, then the amount of remineralized nutrients calculated by (13) is restricted to the bottom interval of the model. An amount of nutrients equivalent to β_s is subtracted from the euphotic zone (β_e in (1a)) following an adjustment to account for the difference in thicknesses of the euphotic and subeuphotic zones.

Any organic carbon flux to the sediments is instantaneously remineralized in the bottom layer of the model. This is in accordance with observations that the amount of organic carbon and other nutrients permanently sequestered in the sediments is small for both marine [*Emerson and Hedges*, 1988] and lacustrine settings [*Schindler et al.*, 1973].

Data used to construct equations such as (11) are generally taken from sediment traps at depths of >100 m [*Berger et al.*,

1989]. The applicability of (11) to aquatic domains of <100 m depth is a point of continuing model evaluation. For most oligotrophic and some mesotrophic settings the compensation depth is >100 m [*Parsons et al.*, 1984], and the transfer of nutrients via (13) is justifiable on the basis of the empirical formulations. For highly productive environments, the compensation depth is usually <100 m because of the light limitation expressed in (6) and (7). In these productive settings, nutrients transferred in the model via (13) to depths above the thermocline tend to be rapidly mixed back into the euphotic zone via turbulent diffusion and thus remain in the biologically active portion of the model. Nutrients transferred to depths below the thermocline and above 100 m are not within the depth range used to construct expressions such as (11) and may therefore be a source of model error.

Empirical constants. The biogeochemical model described by (1)–(13) contains seven empirical constants determined from laboratory field or numerical studies (Table 1) which have no universally accepted values. A standard value for six of the seven constants has been determined by taking median values from seven previously published ecosystem models [*Harleman*, 1977; *Jamart et al.*, 1977; *Kremer and Nixon*, 1978; *Hofmann and Ambler*, 1988; *Wroblewski et al.*, 1988; *Fasham et al.*, 1993; *Ambrose et al.*, 1993] and one book which summarizes a number of ecosystem models and field studies [*Walsh*, 1988] (Table 1). The only constant not established from previous ecosystem models is the remineralization rate, R. A uniform value of R (0.1 d^{-1}) is used in conservation equations of the three model components (equations (1)–(3)). Most other ecosystem models use different remineralization rates for specific particulate components (i.e., phytoplankton, zooplankton, bacteria, organic detritus). Sensitivity analyses discussed in detail below show that changing the remineralization rate has very little effect on the biogeochemical model results.

Choice of a limiting nutrient. Considerable research effort has been directed toward determining the nutrient which limits biological productivity in lakes and oceans. Nitrate is generally believed to be the limiting nutrient in most portions of the ocean [e.g., *Codispoti*, 1989], whereas phosphate limits production in most lakes [*Schindler*, 1977]. Iron may limit phytoplankton growth in high-latitude portions of the ocean [*Martin and Fitzwater*, 1988; *Martin et al.*, 1990].

This study simply employs a generic limiting nutrient (equation (1)), which can represent either phosphorus or nitrate. Once concentrations of the limiting nutrient are exhausted, productivity ceases (equations (4) and (12)).

Model Simplifications and Constraints

Horizontal advection. An obvious potential source of error in the deep water portion of the model arises from the instantaneous transfer of nutrients from the euphotic to subeuphotic zones in conjunction with horizontal advection of dissolved and particulate nutrients (Figure 2). The magnitude of this error depends on the amount of horizontal advection, the depth of the water column, and the actual settling velocity of the particles. Most particle settling velocities are between 1 and 100 m/d [*Smayda*, 1970]. If the settling velocity is relatively low and the water relatively deep (>100 m), then it could take particles as much as 100 days to move from the euphotic zone to deep water. If deep water horizontal velocities are high and particle settling velocities low, then the difference between deep water calculations of a biogeochemical model which spec-

ifies particle settling velocity and a model such as this one which instantaneously transfers the particles through the water column could be significant (Figure 2). Higher particle velocities or shallower water would, of course, reduce this error.

The potential errors in simulations of deep water particulate organic matter are not considered critical since many of the applications envisioned for this model (e.g., simulation of surface productivity as a function of point and nonpoint source nutrient loading) are surface layer phenomena. Spatial errors in the simulation of subeuphotic zone processes (e.g., eutrophication) would be dependent on the particular domain being modeled. Deep water horizontal velocities in most lakes are relatively small (order of centimeters per second) [*Hutchinson*, 1975], so the error in simulating this domain should be relatively minor. Although current velocities over the continental shelf can be high (the order of 1 m/s), water depths are generally <100 m, so this is another domain where the model could probably be used. As mentioned previously, measured particle settling velocities can vary by more than 2 orders of magnitude and are a major source of uncertainty in many aquatic ecosystem models. The model described here thus sacrifices realistic spatial simulations of the deep water domain in order to gain efficient and realistic temporal simulation of surface water processes.

Ammonium and dissolved organic matter. Ammonium and dissolved organic matter (DOM) are not specifically used in this model. The use of these components in previous models and the rationale for excluding them from this model are discussed in detail here. Ammonium (NH_4^+) is a standard component of many biogeochemical models [e.g., *Harleman*, 1977; *Jamart et al.*, 1977; *Wroblewski*, 1977; *Kremer and Nixon*, 1978; *Hofmann and Ambler*, 1988; *Fasham et al.*, 1993; *Ambrose et al.*, 1993], in part because this reduced form of nitrogen is believed to be preferentially taken up by phytoplankton. Photosynthetic uptake of ammonium by phytoplankton is poorly understood, however, and may be dependent on particular species or even the clones within individual species [*Parsons et al.*, 1984]. Although exclusion of ammonium from this study may result in discrepancies in the modeling of some features such as large phytoplankton blooms, it does not appear to be particularly deleterious to the model performance [*Jewell*, this issue].

Considerable recent research in the ocean has focused on the role that DOM plays in biogeochemical cycles. (As used here, DOM includes dissolved organic carbon, nitrogen, and phosphate.) DOM is believed to take two forms: a labile component which enters into the short-term biogeochemical cycles of the euphotic zone, and a refractory component which is more important to long-term geochemical cycles of ocean [e.g., *Suzuki et al.*, 1985; *Sugimura and Suzuki*, 1988; *Toggweiler*, 1989; *Najjar et al.*, 1992]. Recently, *Suzuki* [1993] retracted a previously published high DOM estimate in the ocean [*Suzuki et al.*, 1985; *Sugimura and Suzuki*, 1988], and debate about the role of refractory DOM is very intense [*Wangersky*, 1993]. The importance of the labile fraction of DOM is also somewhat uncertain [*Fasham et al.*, 1990].

DOM is not included in this model because of the uncertainty in analytical techniques and the lack of extensive databases. Several other ecosystem models also do not explicitly model DOM [*Jamart et al.*, 1977; *Kremer and Nixon*, 1978; *Hofmann and Ambler*, 1988; *Wroblewski et al.*, 1988; *Ambrose et al.*, 1993].
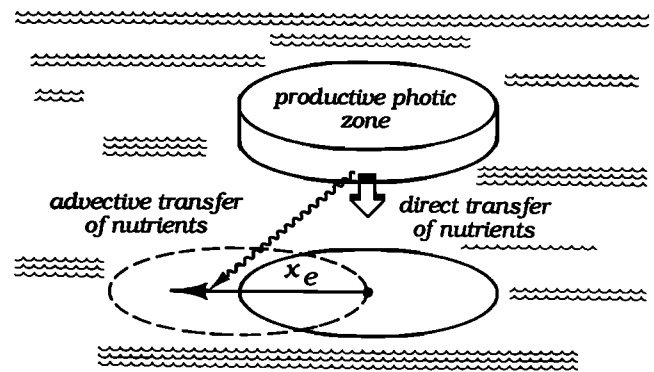

Figure 2. Diagrammatic representation of the spatial error (x_e) associated with the instantaneous transfer of nutrients from the euphotic to the subeuphotic zone in conjunction with horizontal advection in the euphotic zone. The solid circle below the productive photic zone represents the direct transfer of particulate matter by the empirical biogenic particle flux-depth relationships used in the model. The dashed circle is a diagrammatic representation of the actual distribution of particulate matter due to the settling of particles in conjunction with advection of water (right to left in this diagram).

Model Simulations

The three-component biogeochemical model has been coupled to a one-dimensional turbulence closure, fluid flow model and applied to a generalized surface water setting. The generalized model run described here is intended to provide a framework for subsequent model application to specific settings. The model run consists of a 3-year simulation in which the final year of the simulation is saved and plotted. Differences between computed variables of the first and second year were significant, whereas differences between the second and third year simulations were minor.

Fluid Flow Model

A variety of fluid dynamic models have been constructed to simulate vertical mixing in a water column (see review by *Large et al.* [1994]). Algorithms based on Richardson number determinations have been employed in oceanic general circulation models with relatively large grid spacings [e.g., *Pacanowski and Philander*, 1981; *Sarmiento et al.*, 1993]. Other bulk mixed layer models are described by *Krauss and Turner* [1967], *Niiler* [1975], and *Price et al.* [1986].

The fluid flow model used in this study is based on theoretical and laboratory studies of turbulence closure described by *Mellor and Yamada* [1974, 1982]. Other turbulence closure models include *Gaspar et al.* [1990] and *Kantha and Clayson* [1994]. Use of the Mellor-Yamada model for this study is motivated by a desire to produce accurate simulations of vertical eddy diffusivity and the mixing of various biogeochemical components at detailed spatial and temporal scales. The Mellor-Yamada model solves all components of the Reynolds stress equations either analytically or empirically in order to calculate eddy viscosity and diffusivity.

One-dimensional versions of the Mellor-Yamada model have been previously applied to the study of seasonal temperature [*Mellor and Durbin*, 1975] and nutrient [*Klein and Coste*, 1984] variation in the marine mixed layer and a study of anoxia in shallow lakes [*Jewell*, 1992]. Three-dimensional versions of the Mellor-Yamada model have been successfully applied to a

Table 2. Summary of Variables Used in the Generalized Model

Variable	Model Symbol	Value
Depth, m	H	100
Latitude, degrees	...	40
Minimum temperature (mid-January), °C	...	4
Maximum temperature (mid-July), °C	...	20
Initial nutrient concentration, mmol/m³	N_I	1.0 NO$_3^-$
Maximum wind strength, m/s	A	14
Cloudiness, %	C_I	0.5

variety of marine and estuarine settings [e.g., *Oey et al.*, 1985a, b, c; *Mellor and Kantha*, 1989; *Galperin and Mellor*, 1990a, b; *Jewell et al.*, 1993]. A detailed description of numerical implementation of the Mellor-Yamada model can be found in other references [*Blumberg and Mellor*, 1987; *Conner*, 1991] and is not provided here. At mesoscale (1–100 km) dimensions, the Mellor-Yamada model is widely recognized as an important tool for studying the response of surface water flow to winds and solar heating [*Martin*, 1985; *American Society of Civil Engineers, Task Committee on Turbulence Models in Hydraulic Computations*, 1988; *Large et al.*, 1994].

Boundary Conditions and Numerical Implementation

Boundary conditions for the simulations are either fixed values or fluxes. The surface temperature boundary condition is specified as a seasonally varying sine wave. Temperature could be computed as a heat flux boundary condition which is a function of surface air temperature, wind speed, relative humidity, and barometric pressure. This procedure is a standard feature of many surface water models [e.g., *Mellor and Kantha*, 1989; *Hostetler and Bartlein*, 1990] and will be incorporated into future versions of the hybrid fluid dynamic–biogeochemical model. Since the specific purpose of this paper is evaluation of the biogeochemical model, the simpler fixed-temperature boundary condition is used. Bottom boundary heat flux was set to 60 mW/m², an average value for continental heat flow [e.g., *Press and Sevier*, 1978]. Zero-flux conditions for the geochemical components were used at both top and bottom boundaries.

The surface momentum boundary conditions for the one-dimensional model were specified according to the relationship

$$(-\overline{wu}, \; -\overline{wv})_{z=0} = A\left(\sin \frac{2\pi t}{T}, \; \sin \frac{2\pi t}{T} \right) \qquad (14)$$

where $\overline{wu}$ and $\overline{wv}$ are horizontal Reynolds shear stresses, t is time, T is 1 day, and A is maximum daily wind stress (Table 2). The diurnal variation in wind direction implied by (14) is meant to simulate the time-varying kinetic energy input at the air-water interface. Of course, natural wind over most aquatic (particularly marine settings) seldom has diurnal variation. The purpose of this study was to evaluate the performance of a new biogeochemical model using realistic, but idealized, physics, and so this method of time-varying wind stress is considered acceptable.

The fluid dynamic and biogeochemical equations are solved with an implicit finite difference scheme in the vertical dimension and a leapfrog time-differencing scheme [*Mellor and Durbin*, 1975]. The model runs described below used 40 verti-

cal grid points with logarithmic spacing in the upper three grid points and equal grid spacing elsewhere. The time step was 30 min. The effect of changing the time step and grid spacing is discussed below. A 1-year simulation of 40 grid points requires approximately 7 min of CPU time on a Sun Sparc 4/330 workstation, with approximately 60% of the computational effort being devoted to the fluid dynamic model and 40% to the biogeochemical model.

Sensitivity Analyses

Sensitivity analyses were conducted for the model time step and grid spacing (Table 3), as well as the seven empirical constants used in the biogeochemical model (Table 4). For each sensitivity analysis simulation a vertically integrated annual average productivity was calculated for comparative purposes.

Changing the grid spacing and time step changed the model output very little. Vertically integrated surface productivity varied by no more than 10% as the time step was varied from 15 min to 2 hours and the number of grid points varied from 20 to 80 (Table 3). Concentrations of individual chemical components showed higher variability at low concentrations. All physical and chemical variables showed the same spatial and temporal patterns regardless of the time step and grid spacing.

Changing four of the seven parameters in the biogeochemical model (maximum zooplankton growth rate, Ivlev constant, nutrient half-saturation constant, and remineralization rate) produced relatively little change in the integrated productivity (Table 4). Varying the other three parameters (initial slope of the light-productivity curve, light attenuation coefficient, and photosynthetically available radiation) produced rather marked variations in integrated surface productivity. Similar sensitivity of the initial slope of the light-productivity curve is reported by other researchers [*Fasham et al.*, 1990], yet laboratory studies show this parameter to be extremely dependent on phytoplankton species and environmental conditions [*Parsons et al.*, 1984; *Walsh*, 1988]. A constant value for the initial slope of the light-productivity curve is assumed in this model and its applications [*Jewell*, this issue], although this parameter will be a focus of future modeling research. Reported values for the light attenuation coefficient [*Jerlov*, 1976] and PAR [*Fasham et al.*, 1990] are generally in a fairly narrow range, and specifying these parameters is considered less critical. Interestingly, the three most sensitive model parameters all deal with the light regime, while the four relatively insensitive parameters (maximum zooplankton growth rate, Ivlev constant, nutrient half-saturation constant, and remineralization rate) are strictly related to the changes in the biogeochemical variables.

Table 3. Summary of Sensitivity Analyses of Average Annual Productivity Using the Standard Model Parameters (Table 1) for Different Grid Spacing and Time Steps

Number of Grid Points	Time Steps, min			
	15	30	60	120
20	36.1	37.9	38.8	38.1
40	38.0	38.7	39.6	38.6
80	36.1	39.5	39.8	38.3

Values are in g C m^{-2}/yr.

Table 4. Summary of Sensitivity Analyses of the Biogeochemical Model Parameters

Parameter	Symbol	Minimum Value	Minimum Value Integrated Productivity, g C m^{-2}/yr	Maximum Value	Maximum Value Integrated Productivity, g C m^{-2}/yr
Remineralization rate, d^{-1}	R	0.05	45.1	0.20	38.3
Nutrient half-saturation constant, mmol N/m^3	K_p	0.20	42.4	1.0	24.4
Maximum growth rate for zooplankton, d^{-1}	G_{max}	0.10	43.2	0.40	41.7
Ivlev constant, m^3/mmol N	K_I	0.50	42.6	3.0	41.3
Initial slope of light-productivity curve, d^{-1}/W m^{-2}	α	0.010	59.0	0.050	18.6
Photosynthetically active radiation, dimensionless	PAR	0.3	26.7	0.7	47.7
Light attenuation coefficient, m^{-1}	k_w	0.03	52.9	0.05	29.4

Standard values from Table 1 give an average annual productivity of 38.7 g C m^{-2}/yr.

Idealized Model Results

A series of generalized simulations were conducted in order to demonstrate model viability and to investigate the relationship between physical parameters and the biogeochemical response. For the idealized simulation, water depth was 100 m and surface temperature varied as a seasonal sine function between 4° and 20°C (Table 2). The relatively low initial nutrient concentrations (1 mmol/m^3 NO$_3^-$ or 0.06 mmol/m^3

PO$_4^{3-}$) and depth would make this setting typical of an oligotrophic, temperate-latitude lake.

Modeled temperature, vertical eddy diffusivity, nitrate, and chlorophyll all reflect monomictic behavior in which the water column overturns in the late fall (Figure 3). Vertical eddy diffusivity is high in the epilimnion (approximately 10^{-2} m^2/s) and more than 6 orders of magnitude lower in the thermocline and underlying waters (Figure 3b). The low thermocline eddy
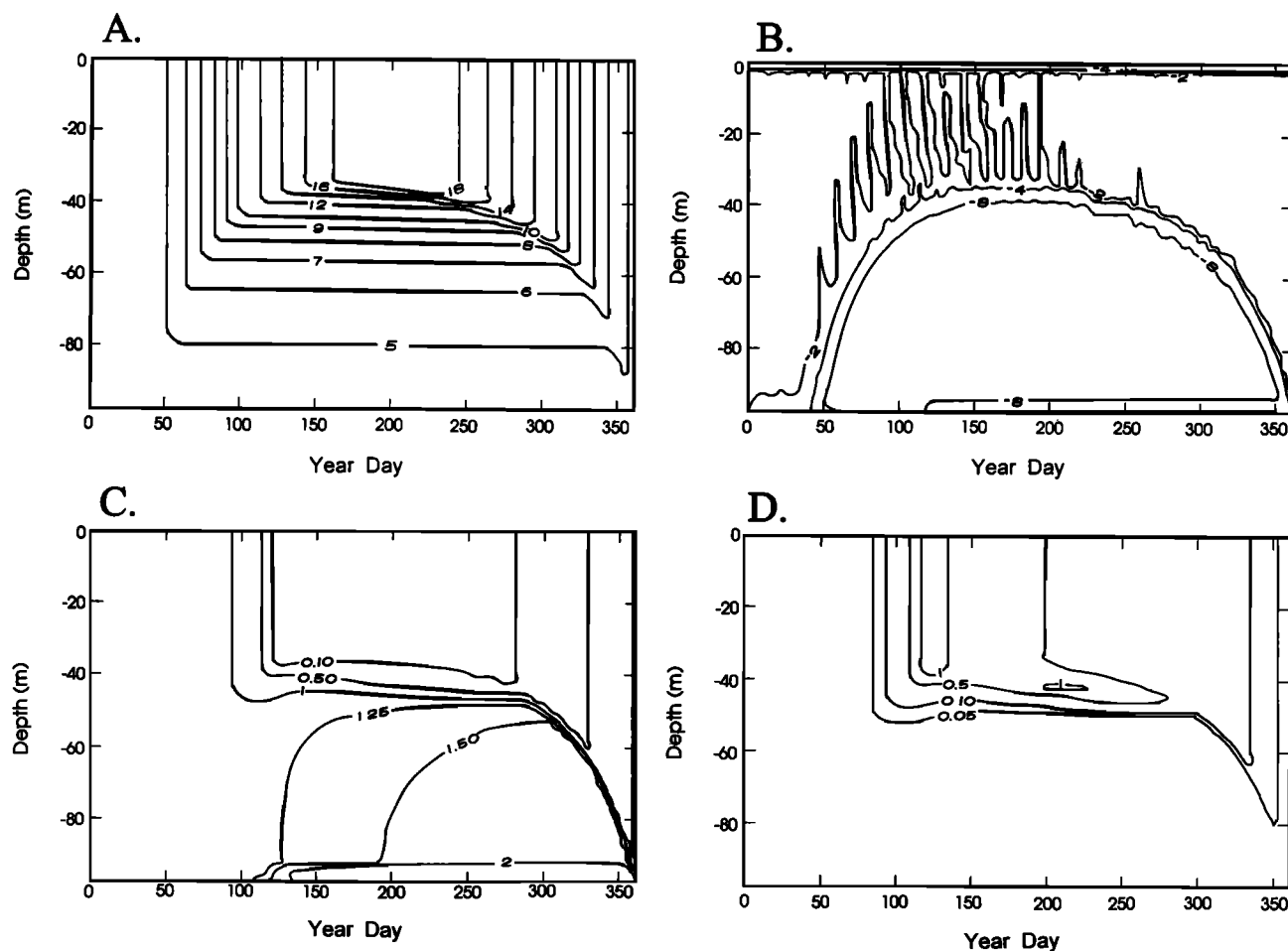

Figure 3. Results from generalized model simulations over a 1-year period: (a) temperature (degrees Celsius); (b) log eddy diffusivity (square meters per second); (c) dissolved nitrate (millimoles per cubic meter); and (d) phytoplankton as chlorophyll a (milligrams per cubic meter).
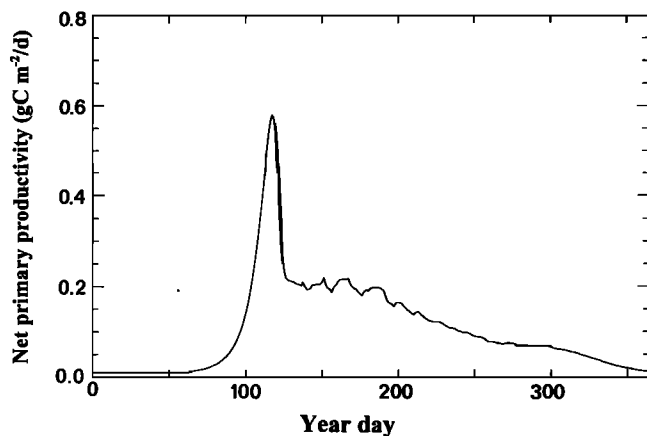
Figure 4. Integrated vertical productivity for the generalized model simulation (g C m^{-2}/yr).

diffusivities calculated by the model are close to molecular diffusivity values [Li and Gregory, 1974] as well as being in general agreement with diffusivities calculated in field localities from nutrient [Imboden and Emerson, 1975] and tritium [Quay et al., 1980] distributions. Very low modeled values of vertical eddy diffusivity in the hypolimnion are somewhat lower than those reported in field studies. This is probably due to the fact that shear stresses caused by internal waves are not reproduced particularly well by the one-dimensional fluid flow model. These shortcomings were noted when modeling sediment biological oxygen demand in seasonally anoxic lakes [Jewell, 1992].

Nitrate concentrations are uniformly distributed through the water column prior to the onset of seasonal stratification (Figure 3c). Nitrate (or phosphate) is reduced to very low values in the epilimnion while there is a commensurate increase in hypolimnitic nitrate as the season progresses. Chlorophyll concentrations likewise are highest during the spring bloom at approximately year day 120 (Figure 3d). Chlorophyll concentrations in the epilimnion reach values of 1 mg/m^3 during the spring bloom and then drop off substantially. In the late summer a deep chlorophyll maximum can be observed immediately above the thermocline (Figure 3d). Vertically integrated productivity (equation (12)) is relatively high during the spring bloom (0.6 g C m^{-2}/yr) and drops off in a regular manner to low (<0.1 g C m^{-2}/yr) values at the end of the year (Figure 4). The late-season deep chlorophyll maximum does not appear to contribute substantively to the integrated productivity.

The occurrence of a deep chlorophyll maximum (DCM) has been noted in studies of Lake Michigan [Brooks and Torke, 1977], Lake Tahoe [Kiefer et al., 1972; Holm-Hansen et al., 1976; Abbott et al., 1984], the Experimental Lakes Area of southern Ontario [Fee, 1976], the Gulf of Mexico [Steele, 1964], the Pacific Ocean [Anderson, 1969, 1972; Saijo et al., 1969; Kiefer et al., 1976; Jamart et al., 1977], the Atlantic Ocean [Hobson and Lorenzen, 1972; Fasham et al., 1993], and the Indian Ocean [Yentsch, 1965; Saijo, 1973]. The origin of the DCM has been attributed to a variety of processes. The intensity of vertical turbulent diffusion influences the nutrient flux and therefore phytoplankton growth rates between the euphotic and subeuphotic zones [Anderson, 1969]. Adaptation of phytoplankton to low light regimes at depth results in an increase in the chlorophyll-to-carbon ratio of cell material and has been offered as an explanation for the DCM [Steele, 1964]. Differential sinking of phytoplankton cells out of the euphotic

zone [Kiefer et al., 1972] and changes in the mortality rate of phytoplankton [Fee, 1976; Fasham et al., 1993] are also possible mechanisms of DCM formation.

Since the model described here does not employ phytoplankton (or any biogenic particle) settling rates, it cannot evaluate all of the DCM formation mechanisms mentioned above. However, the possible importance of vertical mixing to the development of the DCM in this model can be seen in a plot of modeled chlorophyll and vertical eddy diffusivity following the spring overturn (Figure 5). The highest chlorophyll concentrations are associated with eddy diffusivities of greater than 10^{-9} m^2/s. These diffusivities occur immediately above the thermocline (Figure 3b). The relatively high diffusivities and mixing above the thermocline cause a high flux of nutrients upward from the nutrient-rich, late-season hypolimnion, thereby stimulating biological productivity. The DCM in the model is thus a direct result of the highly contrasting values of vertical mixing in the water column. The simulations presented here point out the desirability of using a realistic physical model (such as a turbulence closure model) to accurately simulate eddy viscosity and diffusivity. Vertical eddy diffusivity controls mixing in the water column, which in turn is a key to controlling the biogeochemical processes throughout the water column.

Discussion

A biogeochemical model with an empirical function for transferring nutrients from the euphotic to the subeuphotic zone represents a computationally viable alternative to more complete aquatic ecosystem models. The three-component model with seven empirical constants described here is considerably less complex than many other marine ecosystem models including those presented by Harleman [1977] (seven components and 15 parameters), Hofmann and Ambler [1988] (10 components and approximately 58 parameters), Fasham et al. [1990, 1993] (seven components and 24 parameters), and Ambrose et al. [1993] (eight components and at least 20 parameters). Approximately 40% of the computational resources necessary to run this model are devoted to the three biogeochemical components. Solving the conservation equations for a more complex ecosystem model would clearly lead
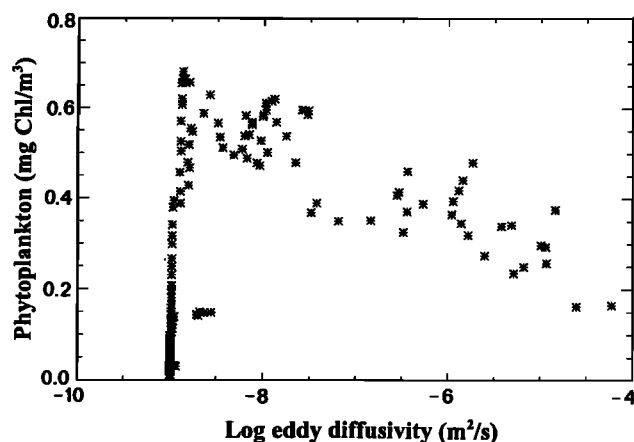

Figure 5. Phytoplankton concentration as chlorophyll a (milligrams per cubic meter) versus eddy diffusivity (square meters per second) for the postspring bloom period (year days 160–260 in Figure 3).

to much higher computational demands which (depending on the goals of the particular application) might or might not be justified.

Coupling the three-component biogeochemical model to a turbulence closure fluid dynamic model produces seasonal simulations of nutrients and phytoplankton which fit the conceptual model of complete water column mixing during the spring, followed by a phytoplankton bloom, nutrient depletion of the euphotic zone, and deep water nutrient enrichment in the summer and fall. Large mixing gradients as shown by vertical eddy diffusivity in the model appear to have a fundamental control on formation of the deep chlorophyll maximum which is a common feature of numerous marine and lacustrine settings.

Although computationally simple, the model described here is not without drawbacks. Certainly, it is not possible to study the fine details of all the possible biogeochemical components found in nature (e.g., bacteria and dissolved organic matter). The model is probably most appropriate for studying phenomena in relatively shallow water regimes such as lakes, estuaries, and marginal marine environments (e.g., continental shelves, inland seas). Research is currently under way to use three-dimensional versions of the model to study the interaction between physics and biogeochemistry in a number of these environments.

References

Abbott, M. R., K. L. Denman, T. M. Powell, P. J. Richerson, R. C. Richards, and C. R. Goldman, Mixing and dynamics of the deep chlorophyll maximum in Lake Tahoe, *Limnol. Oceanogr.*, 29, 862–878, 1984.

Ambrose, R. B., T. A. Wool, and J. L. Martin, The water quality analysis simulation program, WASP5, report, 203 pp., Environ. Res. Lab., Environ. Prot. Agency, Athens, Ga., 1993.

American Society of Civil Engineers, Task Committee on Turbulence Models in Hydraulic Computations, Turbulence modeling of surface water flow and transport, III, *J. Hydraul. Eng.*, 114, 1015–1033, 1988.

Anderson, G. C., Subsurface chlorophyll maximum in the northeast Pacific Ocean, *Limnol. Oceanogr.*, 14, 386–391, 1969.

Anderson, G. C., Aspects of marine phytoplankton studies near the Columbia River, with special reference to a subsurface chlorophyll maximum, in *The Columbia River Estuary and Adjacent Ocean Waters: Bioenvironment Studies*, edited by A. T. Pruter and D. L. Alverson, pp. 219–240, Univ. of Wash. Press, Seattle, 1972.

Bacastow, R., and E. Maier-Reimer, Ocean circulation model of the carbon cycle, *Clim. Dyn.*, 4, 95–125, 1990.

Bacastow, R. and E. Maier-Reimer, Dissolved organic carbon in modeling oceanic new production, *Global Biogeochem. Cycles*, 5, 71–85, 1991.

Berger, W. H., K. Fisher, C. Lai, and G. Wu, Ocean productivity and carbon flux, I, Overview and maps of primary production and export production, *Ref. 87-30*, Scripps Inst. of Oceanogr., La Jolla, Calif., 1987.

Berger, W. H., V. S. Smetacek, and G. Wefer, Ocean productivity and paleoproductivity—An overview, in *Productivity in the Ocean: Past and Present*, edited by W. H. Berger, V. S. Smetacek, and G. Wefer, pp. 1–34, John Wiley, New York, 1989.

Bishop, J. K. B., Regional extremes in particulate matter composition and flux: Effects on the chemistry of the ocean interior, in *Productivity in the Ocean: Past and Present*, edited by W. H. Berger, V. S. Smetacek, and G. Wefer, pp. 117–137, John Wiley, New York, 1989.

Blumberg, A. F., and G. L. Mellor, A description of a three-dimensional coastal ocean circulation model, in *Three-Dimensional Coastal Circulation Ocean Models, Coastal Estuarine Sci. Ser.*, vol. 4, edited by N. S. Heaps, pp. 1–16, AGU, Washington, D. C., 1987.

Broecker, W. S., *Chemical Oceanography*, 214 pp., Harcourt Brace, Orlando, Fla., 1974.

Brooks, A. S., and B. G. Torke, Vertical and seasonal distribution of chlorophyll *a* in Lake Michigan, *J. Fish. Res. Board Can.*, 34, 2280–2287, 1977.

Codispoti, L. A., Phosphorus vs. nitrogen limitation of new and export production, in *Productivity in the Ocean: Past and Present*, edited by W. H. Berger, V. S. Smetacek, and G. Wefer, pp. 377–394, John Wiley, New York, 1989.

Conner, W. P., A user's manual for the Princeton numerical ocean model, *Spec. Rep. 5*, 69 pp., Inst. for Naval Oceanogr., Stennis Space Center, Miss., 1991.

Emerson, S., and J. I. Hedges, Processes controlling the organic carbon content of the open ocean, *Paleoceanography*, 3, 621–634, 1988.

Epply, R. W., Temperature and phytoplankton growth in the sea, *Fish Bull.*, 70, 1063–1085, 1972.

Falkowski, P. G., and C. D. Wirick, A simulation model of the effects of vertical mixing on primary productivity, *Mar. Biol.*, 65, 69–75, 1981.

Fasham, M. J. R., H. W. Ducklow, and S. M. McKelvie, A nitrogen-based model of plankton dynamics in the oceanic mixed layer, *J. Mar. Res.*, 48, 591–639, 1990.

Fasham, M. J. R., J. L. Sarmiento, R. D. Slater, H. W. Ducklow, and R. Williams, Ecosystem behavior at Bermuda "S" and Ocean Weather Station "India": A general circulation model and observational analysis, *Global Biogeochem. Cycles*, 7, 379–415, 1993.

Fee, E. J., The vertical and seasonal distribution of chlorophyll in lakes of the Experimental Lakes Area, northwestern Ontario: Implications for primary production estimates, *Limnol. Oceanogr.*, 21, 767–783, 1976.

Gachter, R. and D. M. Imboden, Lake restoration, in *Chemical Processes in Lakes*, edited by W. Stumm, pp. 363–388, John Wiley, New York, 1985.

Galperin, B., and G. L. Mellor, A time-dependent, three-dimensional model of the Delaware Bay and River system, 1, Description of the model and tidal analysis, *Estuarine Coastal Shelf Sci.*, 31, 231–253, 1990a.

Galperin, B., and G. L. Mellor, A time-dependent three-dimensional model of the Delaware Bay and River system, 2, Three-dimensional flow fields and residual circulation, *Estuarine Coastal Shelf Sci.*, 31, 255–281, 1990b.

Gaspar, P., Y. Gregoris, and J.-M. Leferve, A simple eddy kinetic energy model for simulations of the oceanic vertical mixing: Tests at station Papa and Long-Term Upper Ocean Study site, *J. Geophys. Res.*, 95, 16,179–16,193, 1990.

Harleman, D. R. F., Real-time models for salinity and water-quality analyses in estuaries, in *Estuaries, Geophysics, and the Environment*, *Natl. Res. Counc. Stud. Geophys.*, pp. 84–93, Natl. Acad. Press, Washington, D. C., 1977.

Higgins, J. M., and B. R. Kim, DO model for discharge from deep impoundments, *J. Environ. Eng. Div. Am. Soc. Civ. Eng.*, 108(EE1), 107–122, 1982.

Hobson, L. A., and C. J. Lorenzen, Relationships of chlorophyll maximum to density structure in the Atlantic Ocean and Gulf of Mexico, *Deep Sea Res.*, 19, 297–306, 1972.

Hofmann, E. E., Plankton dynamics on the outer southeastern U.S. continental shelf, III, A coupled physical-biological model, *J. Mar. Res.*, 46, 919–946, 1988.

Hofmann, E. E., and J. W. Ambler, Plankton dynamics on the outer southeastern U.S. continental shelf, II, A time dependent biological model, *J. Mar. Res.*, 46, 883–917, 1988.

Holm-Hansen, O., C. R. Goldman, R. Richards, and P. M. Williams, Chemical and biological characteristics of a water column in Lake Tahoe, *Limnol. Oceanogr.*, 21, 548–562, 1976.

Hostetler, S. W., and P. J. Bartlein, Simulation of lake evaporation with application to modeling lake level variations of Harney-Malheur Lake, Oregon, *Water Resour. Res.*, 26, 2603–2612, 1990.

Hutchinson, G. E., *A Treatise on Limnology*, 1015 pp., John Wiley, New York, 1975.

Imboden, D. M., Phosphorus model of lake eutrophication, *Limnol. Oceanogr.*, 19, 297–304, 1974.

Imboden, D. M., and S. Emerson, Natural radon and phosphorus as limnologic tracers, *Limnol. Oceanogr.*, 20, 77–90, 1975.

Ivlev, V. S., The biological productivity of waters, *Usp. Sovrem. Biol.*, *19*, 98–120, 1945.

Jamart, B. M., D. F. Winter, K. Bause, G. C. Anderson, and R. K. Lam, A theoretical study of phytoplankton growth and nutrient distribution in the Pacific Ocean off the northwestern U.S. coast, *Deep Sea Res.*, *24*, 753–773, 1977.

Jerlov, N. G., *Marine Optics*, 231 pp., Elsevier, New York, 1976.

Jewell, P. W., Hydrodynamic controls of anoxia in shallow lakes, in *Productivity, Accumulation, and Preservation of Organic Matter: Recent and Ancient Sediments*, edited by J. Whelan and J. Farmington, pp. 201–228, Columbia Univ. Press, New York, 1992.

Jewell, P. W., Deep water nutrient and oxygen gradients in a modern coastal upwelling zone and their paleoceanographic implications, *J. Geophys. Res.*, *99*, 7845–7850, 1994a.

Jewell, P. W., Mass balance models of Ekman transport and nutrient fluxes in coastal upwelling zones, *Global Biogeochem. Cycles*, *8*, 165–177, 1994b.

Jewell, P. W., A simple surface water biogeochemical model, 2, Simulation of selected lacustrine and marine settings, *Water Resour. Res.*, this issue.

Jewell, P. W., R. F. Stallard, and G. L. Mellor, Numerical models of bottom shear stress and sediment distribution on the Amazon continental shelf, *J. Sediment. Petrol.*, *63*, 943–945, 1993.

Kantha, L. H., and C. A. Clayson, An improved mixed layer model for geophysical applications, *J. Geophys. Res.*, *99*, 25,235–25,266, 1994.

Kiefer, D. A., O. Holm-Hansen, C. R. Goldman, R. Richards, and T. Berman, Phytoplankton in Lake Tahoe: Deep-living populations, *Limnol. Oceanogr.*, *17*, 418–422, 1972.

Kiefer, D. A., R. J. Olsen, and O. Holm-Hansen, Another look at nitrate and chlorophyll maxima in the central Pacific, *Deep Sea Res.*, *23*, 1199–1208, 1976.

Klein, P., and B. Coste, Effects of wind stress variability on nutrient transport into the mixed layer, *Deep Sea Res.*, *31*, 21–37, 1984.

Krauss, E. B., and J. S. Turner, A one-dimensional model the seasonal thermocline, II, The general theory and its consequences, *Tellus*, *19*, 98–105, 1967.

Kremer, J. N., and S. W. Nixon, *A Coastal Marine Ecosystem*, 217 pp., Springer-Verlag, New York, 1978.

Large, W. G., J. C. McWilliams, and S. C. Doney, Oceanic vertical mixing: A review and a model with a nonlocal boundary layer parameterization, *Rev. Geophys.*, *32*, 363–403, 1994.

Li, Y.-H., and S. Gregory, Diffusion of ions in seawater and in deep sea sediments, *Geochim. Cosmochim. Acta*, *38*, 703–714, 1974.

Maier-Reimer, E., and K. Hasselman, Transport and storage of CO_2 in the ocean—An inorganic ocean circulation model, *Clim. Dyn.*, *2*, 63–90, 1987.

Martin, J. H., and S. E. Fitzwater, Iron deficiency limits phytoplankton growth in the northeast Pacific Subarctic, *Nature*, *331*, 341–343, 1988.

Martin, J. H., G. A. Knauer, D. M. Karl, and W. W. Broenkow, VERTEX: Carbon cycling in the northeast Pacific, *Deep Sea Res.*, *34*, 267–285, 1987.

Martin, J. H., R. M. Gordon, and S. E. Fitzwater, Iron in Antarctic waters, *Nature*, *345*, 156–158, 1990.

Martin, P. J., Simulation of the mixed layer at OWS November and Papa with several models, *J. Geophys. Res.*, *90*, 903–916, 1985.

Mellor, G. L., and P. A. Durbin, The structure and dynamics of the ocean surface mixed layer, *J. Phys. Oceanogr.*, *5*, 718–728, 1975.

Mellor, G. L., and L. Kantha, An ocean-ice model, *J. Geophys. Res.*, *94*, 10,937–10,954, 1989.

Mellor, G. L., and T. Yamada, A hierarchy of turbulence closure models for planetary boundary layers, *J. Atmos. Sci.*, *31*, 1791–1806, 1974.

Mellor, G. L., and T. Yamada, Development of a turbulence closure model for geophysical fluid problems, *Rev. Geophys.*, *20*, 851–875, 1982.

Michaelis, L., and M. L. Menten, Der Kinetic der Inverteinwirkung, *Biochem. Z.*, *49*, 333–369, 1913.

Monod, J., *Recherches sur la croissance des cultures bacteriennes*, Hermann, Paris, 1942.

Najjar, R. G., J. L. Sarmiento, and J. R. Toggweiler, Downward transport and fate of organic matter in the ocean: Simulations with a general circulation model, *Global Biogeochem. Cycles*, *6*, 45–76, 1992.

Niiler, P. P., Deepening of the wind mixed layer, *J. Mar. Res.*, *33*, 405–422, 1975.

Oey, L.-Y., G. L. Mellor, and R. I. Hires, A three-dimensional simulation of the Hudson-Raritan estuary, I, Description of the model and model simulations, *J. Phys. Oceanogr.*, *15*, 1676–1692, 1985a.

Oey, L.-Y., G. L. Mellor, and R. I. Hires, A three-dimensional simulation of the Hudson-Raritan estuary, II, Comparison with observation, *J. Phys. Oceanogr.*, *15*, 1693–1709, 1985b.

Oey, L.-Y., G. L. Mellor, and R. I. Hires, A three-dimensional simulation of the Hudson-Raritan estuary, III, Salt flux analyses, *J. Phys. Oceanogr.*, *15*, 1711–1720, 1985c.

Pacanowski, R. C., and S. G. H. Philander, Paramerterization of vertical mixing in numerical models of tropical oceans, *J. Phys. Oceanogr.*, *11*, 1443–1451, 1981.

Parkinson, C. L., and W. M. Washington, A large-scale numerical model of sea ice, *J. Geophys. Res.*, *84*, 311–337, 1979.

Parsons, T. R., M. Takahashi, and B. Hargrave, *Biological Oceanographic Processes*, 330 pp., Pergamon, New York, 1984.

Peterson, D. H., and J. F. Festa, Numerical simulation of phytoplankton productivity in partially mixed estuaries, *Estuarine Coastal Shelf Sci.*, *19*, 563–589, 1984.

Pingree, R. D., P. M. Holligan, and G. T. Mardell, The effects of vertical stability on phytoplankton distributions in the summer on the northwest European shelf, *Deep Sea Res.*, *25*, 1011–1028, 1978.

Platt, T., Local phytoplankton abundance and turbulence, *Deep Sea Res.*, *19*, 183–187, 1972.

Press, F., and R. Sevier, *Earth*, 649 pp., Freeman, New York, 1978.

Price, J. F., R. A. Weller, and R. Pinkel, Diurnal cycling: Observations and models of the upper ocean response to diurnal heating, cooling, and wind mixing, *J. Geophys. Res.*, *91*, 8411–8427, 1986.

Quay, P. D., W. S. Broecker, R. H. Hesslein, and D. W. Schindler, Vertical diffusion rates determined by tritium tracer experiments in the thermocline and hypolimnion of two lakes, *Limnol. Oceanogr.*, *25*, 201–218, 1980.

Riley, G. A., Oceanography of Long Island Sound, 1952–1954, IX, Production and utilization of organic matter, *Bull. Bingham Oceanogr. Coll.*, *15*, 324–343, 1956.

Saijo, Y., The formation of the chlorophyll maximum in the Indian Ocean, in *The Biology of the Indian Ocean*, edited by B. Zeitzschel and S. A. Gerlack, pp. 171–173, Springer-Verlag, New York, 1973.

Saijo, Y., S. Iizuka, and O. Asaoka, Chlorophyll maxima in Kuroshio and adjacent areas, *Mar. Biol.*, *4*, 190–196, 1969.

Sarmiento, J. L., T. D. Herbert, and J. R. Toggweiler, Causes of anoxia in the world ocean, *Global Biogeochem. Cycles*, *2*, 115–128, 1988a.

Sarmiento, J. L., T. D. Herbert, and J. R. Toggweiler, Mediterranean nutrient balance and episodes of anoxia, *Global Biogeochem. Cycles*, *2*, 427–444, 1988b.

Sarmiento, J. L., R. D. Slater, M. J. R. Fasham, H. W. Ducklow, J. R. Toggweiller, and G. T. Evans, A seasonal three-dimensional ecosystem model of nitrogen cycling in the North Atlantic euphotic zone, *Global Biogeochem. Cycles*, *7*, 417–450, 1993.

Schindler, D. W., Evolution of phosphorus limitation in lakes, *Science*, *195*, 260–262, 1977.

Schindler, D. W., H. Kling, R. V. Schmidt, J. Prokopowich, V. E. Frost, R. A. Reid, and M. Capal, Eutrophication of lake 227 by addition of phosphate and nitrate: The second, third, and fourth years of enrichment, 1970, 1971, and 1972, *J. Fish. Res. Board Can.*, *30*, 1415–1440, 1973.

Shaffer, G., A model of biogeochemical cycling of phosphorus, nitrogen, oxygen, and sulfur in the ocean: One step toward a global climate model, *J. Geophys. Res.*, *94*, 1979–2004, 1989.

Smayda, T. J., The suspension and sinking of phytoplankton in the sea, *Oceanogr. Mar. Biol. Annu. Rev.*, *8*, 353–414, 1970.

Smith, E. L., Photosynthesis in relation to light and carbon dioxide, *Proc. Nat Acad. Sci. U.S.A.*, *22*, 504–511, Washington, 1936.

Snodgrass, W. J., and C. R. O'Melia, Predictive model for phosphorus in lakes, *Environ. Sci. Technol.*, *9*, 937–944, 1975.

Southam, J. R., W. H. Peterson, and G. W. Brass, Dynamics of anoxia, *Palaeogeogr. Palaeoclimatol. Palaeoecol.*, *40*, 183–198, 1982.

Steele, J. H., A study of production in the Gulf of Mexico, *J. Mar. Res.*, *22*, 211–222, 1964.

Suess, E., Particulate organic carbon flux in the oceans: Surface productivity and oxygen utilization, *Nature*, *288*, 260–263, 1980.

Sugimura, Y., and Y. Suzuki, A high temperature catalytic oxidation method for the determination of non-volatile dissolved organic carbon in seawater by direct injection of liquid sample, *Mar. Chem.*, *24*, 105–131, 1988.

Suzuki, Y., On the measurement of DOC and DON in seawater, *Mar. Chem.*, *41*, 287–288, 1993.

Suzuki, Y., Y. Sugimara, and T. Itoh, A catalytic oxidation method for the determination of total nitrogen in dissolved seawater, *Mar. Chem.*, *16*, 83–97, 1985.

Toggweiler, J. R., Is the downward dissolved organic matter (DOM) flux important in carbon transport?, in *Productivity in the Ocean: Past and Present*, edited by W. H. Berger, V. S. Smetacek, and G. Wefer, pp. 65–83, John Wiley, New York, 1989.

Walsh, J. J., A spatial simulation of the Peruvian upwelling ecosystem, *Deep Sea Res.*, *22*, 201–236, 1975.

Walsh, J. J., *On the Nature of Continental Shelves*, 520 pp., Academic, San Diego, Calif., 1988.

Walsh, J. J., D. A. Dieterle, and M. B. Meyers, A simulation analysis of the fate of phytoplankton within the Mid-Atlantic Bight, *Cont. Shelf Res.*, *8*, 757–787, 1988.

Wangersky, P. J., Dissolved organic carbon: A critical review, *Mar. Chem.*, *41*, 61–74, 1993.

Wroblewski, J. S., A model of phytoplankton plume formation during variable Oregon upwelling, *J. Mar. Res.*, *35*, 357–394, 1977.

Wroblewski, J. S., J. L. Sarmiento, and G. R. Flierl, An ocean basin scale model of plankton dynamics in the North Atlantic, 1, Solutions for the climatological oceanographic conditions in May, *Global Biogeochem. Cycles*, *2*, 199–218, 1988.

Yentsch, C. S., Distribution of chlorophyll and phaeophytin in the open ocean, *Deep Sea Res.*, *12*, 653–666, 1965.

P. W. Jewell, Department of Geology and Geophysics, 717 W. C. Browning Building, University of Utah, Salt Lake City, UT 84112-1183.